ISBN: 978-3-95450-231-8 ISSN: 2673-5490 doi: 10.18429/JACoW-IPAC2023-WEPL160

LOSS SIMULATIONS ON SHIELDING FOIL SLIT ERRORS

Paul Volz *, A. Meseck , HZB, Berlin, JGU, Mainz, Germany

Abstract

The worldwide first in-vacuum elliptical undulator, IVUE32, is being developed at Helmholtz-Zentrum Berlin. The 2.5 m long device with a period length of 3.2 cm and a minimum gap of about 7 mm is to be installed in the BESSY II storage ring. The device follows the APPLE-II design and features four magnet rows. Both the two bottom and two top rows can be shifted longitudinally. This shift needs to be permitted by the shielding foils that cover the permanent magnets. The proposed solution calls for a longitudinal slit in the top and bottom shielding foils, which gets folded into the gap between the top and bottom magnet rows respectively. The manufacturer states that the folding process can introduce a small sinusoidal error to the slit width. We will present wakefield simulation studies that investigate the effect of different possible foil gap variations.

INTRODUCTION

The APPLE-II design of IVUE32 features four individually movable magnet rows that allow for a shift in polarization of the undulator radiation. A schematic of the proposed magnet assembly is shown in Fig. 1 with the functional magnets highlighted in orange. The shielding foils will cover the functional magnets and will be folded into the gap between the magnet rows. The resulting longitudinal slit is needed to accommodate the shift of the magnets. Further details of the proposed design can be found in a status update by J. Bahrdt *et al.* [1]. This geometry has not yet been investigated. In particular, the wakefields and impedances generated by the passage of electrons through such an geometry may be different from those generated in existing planar in-vacuum undulators. A large, gap-dependent increase in wakefields and impedances can prevent the insertion device (ID) from operating as intended. Thus, the impact of the slit on wakefield and impedance needs to be investigated. The manufacturer has outlined possible errors that can occur during the foil bending process that could affect the geometry and width of the resulting slit. In the following sections we will present wakefield and loss simulations that investigate the impact of the shielding foil geometry and certain variations from the planned geometry.

MODELLING

The shielding foils have been simulated using the wakefield solver of CST Studio Suite [2]. Since the skin depth for the expected frequency range from 1 GHz to 20 GHz is less than 2.5 µm, the nickel-copper foils have been modelled as pure copper sheets with a thickness of 10 µm. The foils are modelled in vacuum with open boundary conditions. One meter of foil structure has been simulated for each case. The gap between the top and bottom foil is 6 mm. The slit in the foil starts after 20 mm and also ends 20 mm before the structure ends. This means that the left and right side of the foil slits are connected at the beginning and exit of the structure. Shifting the magnet rows longitudinally moves the shielding foils and their deviations, leading to a change in slit geometry. According to the manufacturer sinusoidal deviations can be expected during the bending process. Therefore, two different types of sinusoidal errors have been investigated. The first is a symmetric sinusoidal variation of the slit width (symmetric error). The second error is an asymmetric sinusoidal modulation, keeping the slit width constant at 1 mm (asymmetric error). A schematic top view of both cases is shown in Fig. 2. The asymmetric errors are described by

$$x(t) = A \sin\left(\frac{t}{n}\right) \tag{1}$$

where A is the amplitude and n is a quotient governing the period length. The beam parameters used for the simulation correspond to the single bunch operation at BESSY II, the bunch with the highest charge in regular operation. The solver was run with a Gaussian beam with a bunch charge $Q = 10.4$ nC and $\sigma_z = 10.2$ mm. The mesh resolution in the transverse direction was set at 80 cells per wavelength. The longitudinal resolution was set at 80 lines per σ_z.

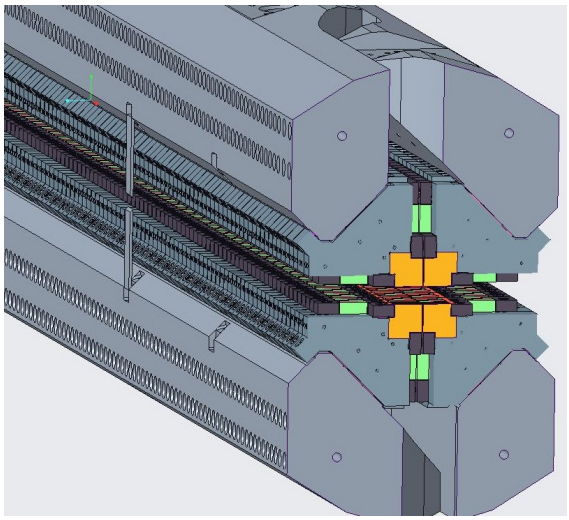

Figure 1: Technical drawing of the proposed IVUE32 magnet assembly. The functional magnets are shown in orange and will be covered by the shielding foil.

SIMULATION

The main concern is energy deposition into the shielding foils. The simulation studies were focused on the Ohmic losses in the shielding foils for different slit geometries, in order to establish tolerances for the manufacturing process.

* paul.volz@helmholtz-berlin.de

ISBN: 978-3-95450-231-8 ISSN: 2673-5490 doi: 10.18429/JACoW-IPAC2023-WEPL160

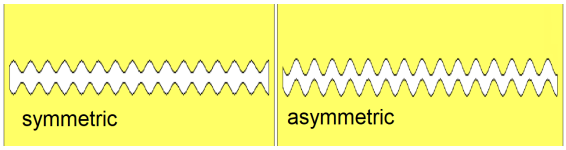

Figure 2: Schematic top view of slit geometry in shielding foils. Symmetric sinusoidal variations of the slit width on the left, asymmetric sinusoidal modulation of slit with constant width of 1 mm on the right.

Figure 3 compares the Ohmic losses of the two error types shown in Fig. 2 with a perfectly straight slit of 1 mm width and a shielding foil with no slit at all. The power losses for the straight slit quickly plateau at around 183 W as the electron beam enters the structure, stay constant as the beam traverses the shielding foils, and decay quickly as the beam exits the structure. This is very similar to the case without a slit. Here the power losses are slightly lower, as the cross section of the conductive material is increased. The losses for the symmetric error show similar characteristics with the addition of a 9.6 W modulation of the losses as the beam traverses the shielding foils. This power loss modulation corresponds to the modulation of the slit width. In the case of the asymmetric error we also see the modulation in power loss but with a growing amplitude. Such a modulation in energy deposition is a serious concern as it can cause hot spots in the shielding foils. This can cause the foil to bulge out due to thermal expansion, which in turn causes further heating due to increasing wakefields. This runaway effect can lead to melting of the foil, as was reported at SOLEIL [3].

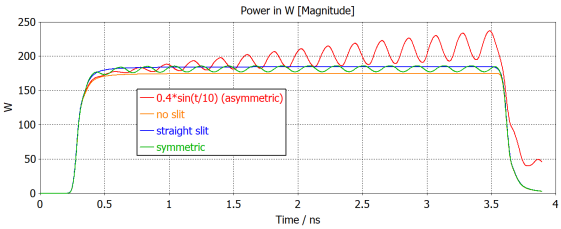

Figure 3: Ohmic losses in the shielding foils for different slit geometries. The asymmetric error shows an increase in power loss for each period. The modulations in loss correspond to the period length of the geometric errors.

The longitudinal wake impedance of the different slit geometries is shown in Fig. 4. We see a fairly flat response across the frequency range for the perfect slit, the foils with no slit, and the symmetric error. The asymmetric error shows resonant behaviour at frequencies around 2.5 GHz, 6.5 GHz, and 10 GHz.

The longitudinal wake potential shown in Fig. 5 for the asymmetric error also differs significantly from the other cases. We can see long range effects out to the simulated wake length of 80 mm, where the other geometries show no significant signal past 60 mm. This would indicates possible coupling between subsequent bunches during multi bunch operation and could disrupt beam stability.

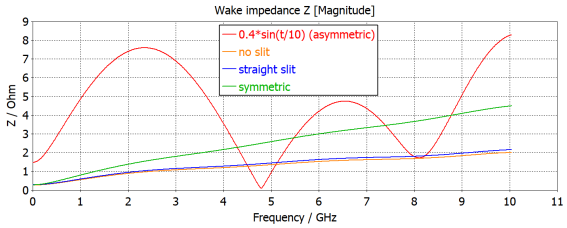

Figure 4: Longitudinal wake impedance for different slit geometries. The straight slit, the symmetric error, and the foils without a slit show a fairly flat response across the frequency range. The asymmetric error shows resonant behaviour around 2.5 GHz, 6.5 GHz, and 10 GHz.

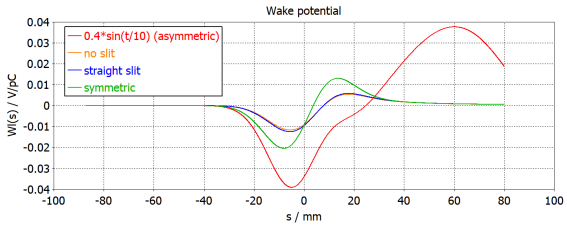

Figure 5: Longitudinal wake potential for different slit geometries. Only the asymmetric error shows a longer ranging potential that could lead to coupling between bunches during multi bunch operation.

Following these results, an asymmetric error in the shielding foil slit seems to be the most disruptive geometry. Further simulations were performed to investigate a change in amplitude and period length of an asymmetric error. Figure 6 shows the Ohmic losses for different amplitudes of asymmetric errors while keeping the period constant. An increase in amplitude also amplifies the calculated losses. Figure 7 shows the maximum value of the calculated Ohmic losses as a function of asymmetric error amplitude. It is difficult to fit an exact function to the relation but the increase in losses is non-linear.

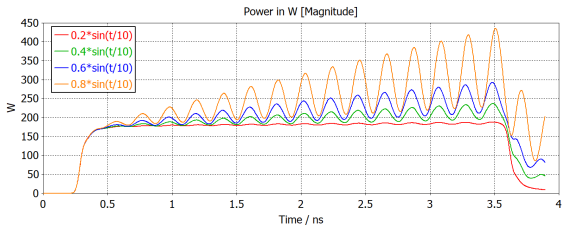

Figure 6: Ohmic losses in the shielding foils for asymmetric errors of different amplitudes with a constant period. The increase in power loss for each error is proportional to its amplitude.

Figure 8 depicts the power loss for three selected period lengths of asymmetric error while keeping the amplitude constant. The modulation of the losses corresponds to the period of the asymmetric error. The difference in loss amplitude is not nearly as pronounced, as in case of a change in error amplitude.

ISBN: 978-3-95450-231-8 ISSN: 2673-5490 doi: 10.18429/JACoW-IPAC2023-WEPL160

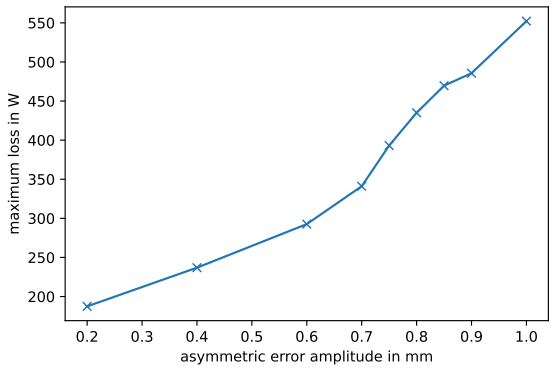

Figure 7: Maximum losses compared for different amplitudes of asymmetric error. Maximum losses increase with the amplitude of the asymmetric error. Growth is non-linear.

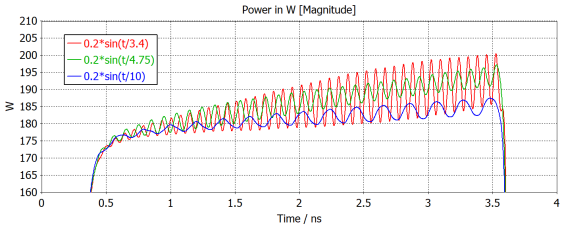

Figure 8: Ohmic losses in the shielding foils for different periods of asymmetric errors with a constant amplitude. The modulation in the losses corresponds to the period of the asymmetric error. Y-axis rescaled for better visibility.

Figure 9 shows the maximum losses as a function of asymmetric error period length. There is an increase in maximum losses indicating a resonant effect corresponding to a period of around 30 mm. There needs to be some caution, however when ascribing a resonance to a certain period length in this case. When simulating structures with curved surfaces, there is a resolution limit in the meshing. Some mesh cells cannot be reasonably aligned with the curved conducting surfaces. CST then fills these cells with a perfect electric conductor (PEC), effectively altering the simulated geometry. The peak in Fig. 9 might be an artefact of the meshing resolution. Further simulations are planned to investigate the impact specific meshing has on the observed effect.
Please note, that the geometry of the asymmetric error is similar to a concept referred to an image charge undulator (ICU) by Y. Zhang *et al.* [4]. A concept that puts a sinusoidal conducting structure very close to a flat electron beam and uses the generated wake field as an undulator field for subsequent bunches. The difference to our simulations is the beam trajectory. In our case of asymmetric errors the ICU-structure is located next to the beam trajectory while in the ICU case the beam trajectory goes directly through the sinusoidal structure. So their findings cannot be directly applied to our case.

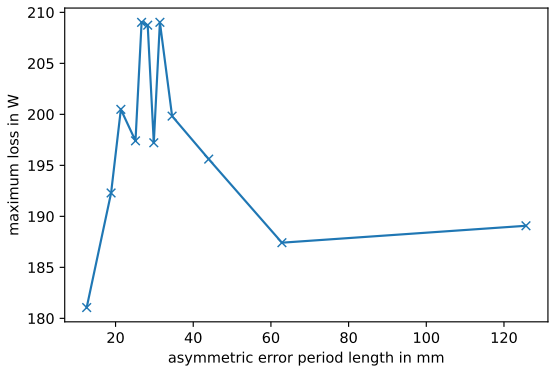

Figure 9: Maximum losses compared for different period lengths of asymmetric errors. Maximum losses show a resonant behaviour corresponding to a period of around 30 mm.

CONCLUSION AND OUTLOOK

The simulations show that periodic modulation of the shielding foil slit geometry can cause growing Ohmic losses and potentially interfere with beam stability. Deviations in slit geometry that are symmetric in the YZ-plane seem to have much less impact on the Ohmic losses and wakefields. The longitudinal shift of the undulator during operation will translate the geometric deviations of the shielding foil on one magnet row with respect to the foil on the other row. This could turn a symmetric error into an asymmetric one at certain shift settings. In order to avoid unstable conditions, the period length of any error in the foil slit should be far greater than the longitudinal travel distance of the magnet rows. The effects of geometric errors on the losses strongly depend on their amplitude. First inquiries to possible foil manufacturers suggest error amplitudes in the order of 0.1 mm are achievable over a 2 m bend. The errors will most likely arise from resetting the bending die as the foils have to be bent in sections. Perfectly periodic errors are also unlikely. This suggests that shielding foils can be manufactured that allow for stable operation of the planned ID.
Further simulations are planned to investigate which effects are physical and which are numerical artefacts resulting from inaccurate meshing. So far the shielding foils have been simulated in a vacuum. The whole undulator structure sits in a cylindrical vacuum chamber. Further simulations of the complete cross section of the structure are planned. Analysing trapped modes and resonances of the complete structure could also be valuable but would differ little from work already done on planar in-vacuum undulators. This work was focused on the new challenges of an in-vacuum APPLE-II structure.

ACKNOWLEDGMENTS

We would like to thank Dr. Erion Gjonaj and Frederik Quetscher for their assistance with the CST simulations, and Dr. Johannes Bahrdt for his feedback on the shielding foil geometries.

ISBN: 978-3-95450-231-8 ISSN: 2673-5490 doi: 10.18429/JACoW-IPAC2023-WEPL160

REFERENCES

[1] J. Bahrdt, J. Bakos, S. Gaebel, S. Gottschlich, S. Grimmer, S. Knaack, *et al.*, "The Status of the In-Vacuum-APPLE II Undulator IVUE32 at HZB / BESSY II", in *Proc. IPAC'22*, Bangkok, Thailand, Jun. 2022, pp. 2716–2718. doi:10.18429/JACoW-IPAC2022-THPOPT052

[2] Dassault Systèmes SIMULIA CST Studio Suite www.3ds.com/products-services/simulia/products/cst-studio-suite

[3] L.S. Nadolski, Y.-M. Abiven, C. Benabderrahmane, P. Brunelle, *et al.*, "Operating Simultaneously Two In-Vacuum Canted Undulators in Synchrotron SOLEIL", in *Proc. 8th Int. Particle Accelerator Conf. (IPAC'17)*, Copenhagen, Denmark, May 2017, paper MOPVA004, pp. 851–854, http://jacow.org/ipac2017/papers/mopva004.pdf, https://doi.org/10.18429/JACoW-IPAC2017-MOPVA004, 2017.

[4] Y. Zhang, Y. Derbenev, *et al.*, "Image charge undulator: theoretical model and technical issues", in *Proceedings of the 2003 Particle Accelerator Conference*, 2003, doi:10.1109/PAC.2003.1289554